Acoustic waves in transversely excited atmospheric CO_2 laser discharges: effect on performance and reduction techniques

Hubertus M. von Bergmann
University of Stellenbosch
LRI
Private Bag X1
Matieland 7602, South Africa
E-mail: hmvb@sun.ac.za

Andrew Forbes, MEMBER SPIE
CSIR National Laser Centre
P.O. Box 395
Pretoria 0001, South Africa
and
University of Kwazulu-Natal
School of Physics
Private Bag X54001
Durban 4001, South Africa

Ted Roberts
Lourens R. Botha
CSIR National Laser Centre
P.O. Box 395
Pretoria 0001, South Africa

Abstract. Results are presented on the influence of acoustic waves on the performance of high-repetition-rate TEA CO_2 lasers. It is shown that acoustic waves generated inside the laser cavity lead to nonuniform discharges, resulting in a deterioration of the laser beam quality, decreased output energy, and an increase in pulse-to-pulse energy variation. The effect of the gas mix on the acoustic behavior is investigated, and experimental results on laser performance across a range of gas mixtures are presented. Methods to reduce the effects of acoustic waves are presented together with experimental results. The influence of acoustic damping measures on laser gain are demonstrated, showing a significant improvement in gain and output power at high pulse repetition rates.
[DOI: 10.1117/1.2968227]

Subject terms: acoustic waves; TEA CO_2 lasers; standing waves; beam quality.

Paper 070965R received Dec. 6, 2007; revised manuscript received Apr. 25, 2008; accepted for publication May 29, 2008; published online Aug. 20, 2008. This paper is a revision of a paper presented at the SPIE conference on Gas Flow, Chemical Lasers, and High-Power Lasers, September 2006, Gmunden Austria. The paper presented there appears (unrefereed) in SPIE Proceedings Vol. 6346.

1 Introduction

Recently there has been renewed interest in TEA CO_2 lasers because of a number of emerging large-scale applications, such as extreme ultraviolet (EUV) generation for photolithography, large-scale paint stripping, and nondestructive testing, e.g., of composite aircraft structures. All of these applications require high average output power with large pulse energies, generally at high pulse repetition rates. Since they are of an industrial nature, long-term reliability and cost effectiveness are of overriding importance. However, since the gain medium for these systems is a gas mix, and since a large amount of energy is deposited into the gas in a short time and at a fixed pulse repetition rate, acoustic waves and shock waves tend to be obstacles to stable performance. In particular, since the energy is deposited into the cavity at a distinct pulse repetition rate, resonantly enhanced standing waves can become a problem.[1–5]

In this paper we report on acoustic wave experiments on two unique TEA CO_2 laser systems. The first [Fig. 1(a)] is a high-pulse-repetition-rate system capable of operating at repetition rates of up to 2000 Hz and delivering up to 2-kW laser output, which was originally developed as an amplifier for molecular-laser isotope separation of uranium by the Nuclear Energy Corporation of South Africa (NECSA). The second system [Fig. 1(b)] studied is a custom-designed laser from Scientific Development and Integration (Pty) Ltd., used extensively for the nondestructive testing of composite materials.[6–8] The laser is capable of 400-Hz operation with very short-duration pulses. The specifications for both lasers require gas mixes that are rich in CO_2 gas (minimum 30% by mole fraction) and consequently experience acoustic problems at lower repetition rates than would be the case with other TEA lasers operating with lean CO_2 gas mixes ($\approx$10% by mole fraction). This is due to the enhanced sensitivity of the discharge to the development of instabilities with the increasing electronegativity of the laser gas at higher CO_2 concentrations. Moreover, the high-pulse-repetition-rate operation of the two systems requires careful design to reduce the deleterious effect of induced acoustic waves.

In Sec. 2 we discuss the experimental laser systems used in this study in more detail, and present the experimental setup used for data gathering. In Sec. 3 we provide results on the acoustic-wave phenomenon in the laser discharge; the effect of the acoustic waves on laser performance, as well as means to reduce this effect, are discussed in Sec. 4.

2 Experimental Systems and Methodology

The internal discharge configuration of the 2000-Hz laser is shown in Fig. 2. The laser employed a wind-tunnel-style flow loop with a centrifugal fan driven by a variable-frequency drive, which provided continuously variable gas flow speeds up to 90 m s^{-1}–fast enough to remove the hot ionized gas from the discharge with sufficient "clearance" prior to the next pulse, up to pulse repetition rates in excess of 2000 Hz. The electrode structure consisted of 800

0091-3286/2008/$25.00 © 2008 SPIE

Fig. 1 (a) The 2000-Hz system, showing the blower system to the left and the laser head to the right. (b) The commercial 400-Hz system designed specifically for laser ultrasonic testing of materials.

×38-mm discharge electrodes (length and width respectively), separated by 20 mm along their length. The laser employed spark preionization by either two arrays of sparks placed up- and downstream of the discharge or a single preionizer row downstream, with a spark separation of 25 mm. Flow guiding profiles, approximating a flow nozzle, provided uniform flow in the discharge region. Arrays of current return feedthroughs were placed up- and downstream of the discharge and distributed along the electrode length with 50-mm spacing. The total energy supplied to the discharge electrodes was 20 J, resulting in a specific energy deposition from 90 to 130 J/(l atm), depending on the gas mixture.

The system was equipped with a number of diagnostic tools, as shown in Fig. 3, to monitor gas dynamics as well as discharge and laser performance. The gas flow velocity was measured with a Pitot tube, and time-resolved pressure measurements were made using fast miniature piezoelectric pressure transducers (PCB model 112 A22, 2-μs rise time). Visual observations of the discharge, both in the gas flow direction and in the direction of the optical axis, were carried out by CCD video cameras through dedicated observation ports. Recordings were made at 24 frames per second; therefore, each video frame was averaged over many discharges. The laser beam quality factor M^2 was measured using the scanning slit method along the propagation axis, following the ISO 11146:1999(E) approach. Arcing in the discharge is often a sign of extreme acoustic disturbances and as such was monitored with a fiber optic collecting light from the discharge region.

Since this work concentrates on the effect of acoustic waves on laser performance, some of the general results are reported without reference to the particular laser system. The laser gas mix was one of the parameters varied in the experiments, and in this paper we adopt the standard notation to describe this, i.e., as mole fractions of CO_2, N_2, and He in the form $CO_2:N_2:He$. Thus 10:10:80 refers to 10 parts CO_2, 10 parts N_2, and 80 parts He.

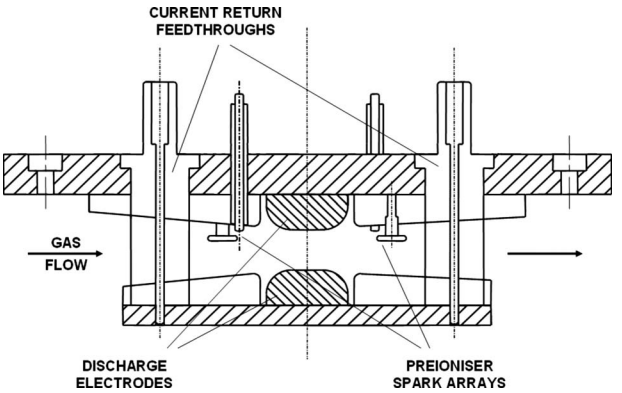

Fig. 2 Electrode configuration in the 2000-Hz system, showing a cross section of the electrodes, the preionization pins (spark arrays), and the feedthroughs. The gas flow is from left to right, and the discharge is the region between the electrodes. The flow-guiding profiles are evident both upstream and downstream of the electrodes.

3 Acoustic Waves in the Discharge

We consider some factors that affect the acoustic waves themselves, such as cavity geometry, laser pulse repetition rate, gas mix, and method of transferring energy into the discharge. Figure 4 shows the discharge appearance recorded side-on in the flow direction. A section of approximately 300-mm length close to the center of the discharge has been imaged. The dark vertical lines are the upstream

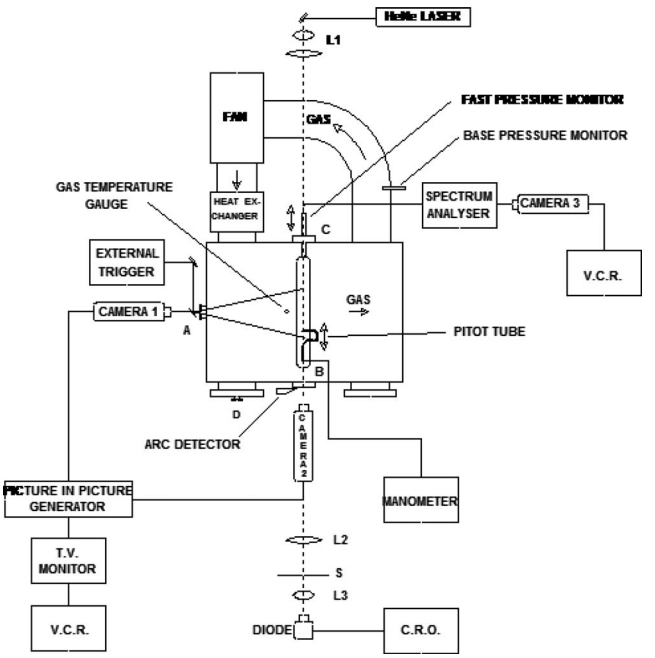

Fig. 3 Diagnostic setup.

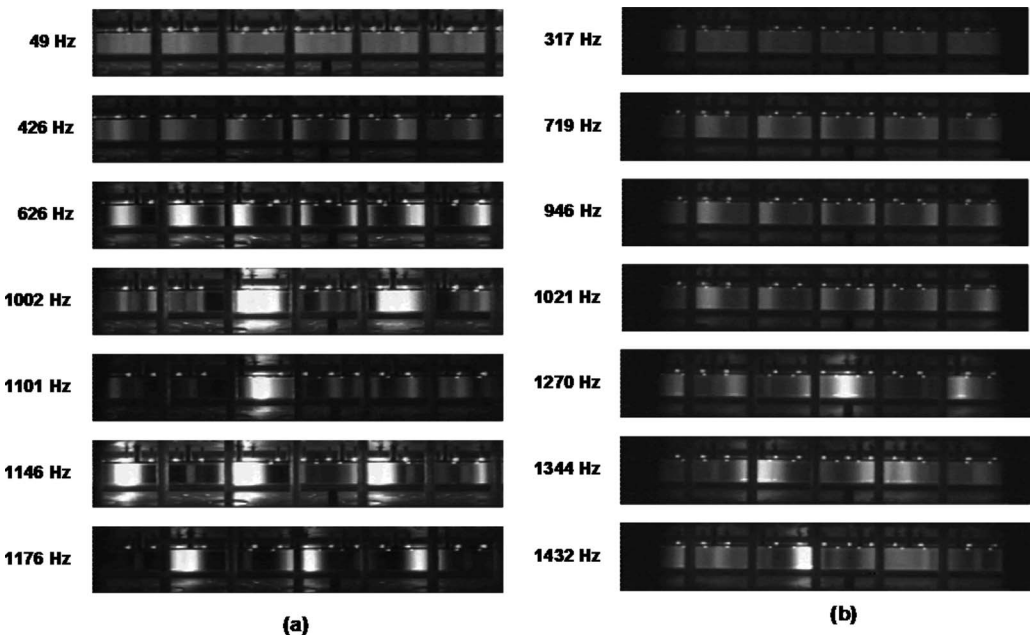

Fig. 4 Transverse discharge appearance for various resonant pulse repetition rates: (a) 36:20:44 and (b) 10:10:80 gas mixes.

current return feedthroughs, and the bright spots at the upper border of the discharge are the preionization sparks. Two gas mixes were considered: a rich 36:20:44 mix [Fig. 4(a)] and a lean 10:10:80 mix [Fig. 4(b)].

At low pulse repetition rates the discharge had a uniform appearance–the so-called *glow discharge*. With the lean gas mix of 10:10:80 this uniform discharge was evident up to very high pulse repetition rates, with acoustic structure only appearing beyond 800 Hz. However, with the 36:20:44 gas mix the discharge became nonuniform along the electrode length as the pulse repetition rate was increased, with some acoustic structure already evident at a repetition rate of 200 Hz, and further increase led to distinctive resonant structures with bright regions behind the feedthroughs (designated *type A* structures), which reappeared at successively higher repetition rates (see for example the 626-Hz image). At higher repetition rates other structures appeared; examples include bright regions behind every second feedthrough (designated *type B* structures) or every third feedthrough (designated *type C* structures) as well as structures displaced by one feedthrough separation or with bright regions between feedthroughs. At very high repetition rates (>1000 Hz) the glow discharge was concentrated in only a few or even one bright current-carrying column, eventually leading to discharge arcing. Similar discharge structures have been observed by other researchers in high-average-power, lower-repetition-rate TEA CO_2 lasers[2] and in high-repetition-rate excimer lasers[9,10] and have been attributed to standing acoustic waves and to pressure fluctuations generated by electrical discharge arcing, respectively. At very high repetition rates there were no frequency regimes with uniform discharges in between resonant structures. Viewing the discharge end on (down the optical axis), we observed contractions of the visible discharge column as well as distinctive sideways shifts. It has been experimentally determined that the appearance of the resonances is largely independent of fan frequency and therefore of gas flow speed.

In general the influence of pulse repetition rate f_L and gas flow velocity v_g on the observed discharge structure can be summarized as follows: At low values of v_g, glow discharges with a relatively uniform intensity distribution along the electrodes are obtained as f_L is increased, until there is a sudden onset of downstream arcing (i.e., arcing from the downstream side of the high-voltage electrode to the grounded downstream structures). This transition can be very sharp (e.g., an increase of the arc/discharge ratio from 1% to 10% for an increase in f_L of as little as 20 Hz). At intermediate v_g, as f_L is increased above a certain value, the discharge exhibits resonant structures along the electrode length. There is no sudden onset of these resonant structures, but rather they appear gradually out of the uniform background intensity as f_L is increased. Also, the discharges between resonances can be relatively uniform. The first arcing is now interelectrode rather than downstream. However, f_L can be further increased with interelectrode arcing at a relatively low level until the onset of downstream arcing. As in the case of low v_g, the increase of downstream arcing rate with increasing f_L is then very rapid. If f_L is increased at high flow rates v_g, all the dominant visible features occur at essentially the same pulse repetition rates, as with lower v_g. However, the threshold frequencies for interelectrode and downstream arcing are increased. Further, at the higher f_L there are practically no frequency intervals with relatively benign discharges.

We have analyzed the acoustic-wave frequency spectrum using a fast piezoelectric pressure transducer and spectrum analyzer. The measured Fourier power spectrum for a pulse repetition rate of 626 Hz [type A structure from Fig. 4(a)] is shown in Fig. 5. The detector was placed at the laser output window, and was therefore primarily measuring acoustic waves transverse to the gas flow, along the

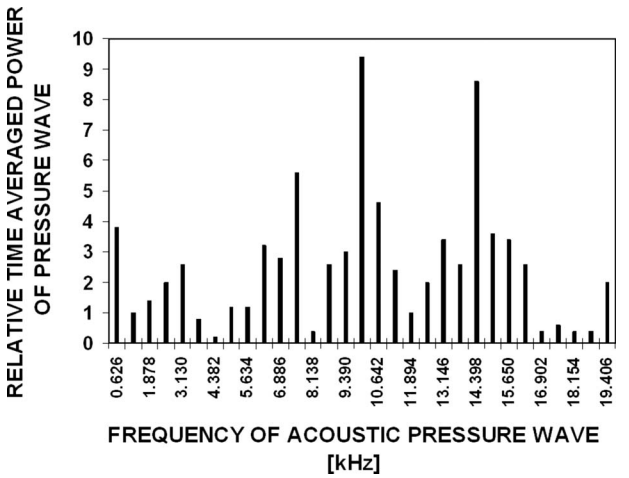

Fig. 5 Cavity resonances excited at a pulse repetition rate of 626 Hz by successive harmonics for $n=1$ to 31.

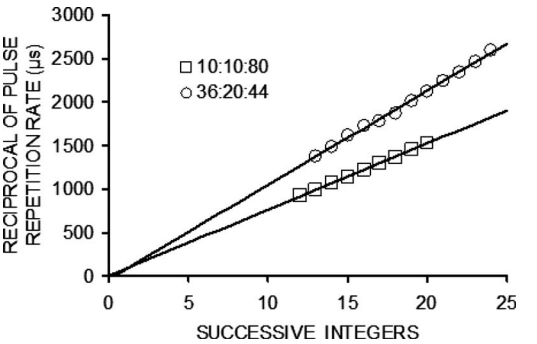

Fig. 6 Reciprocal of frequency of maximum contrast of successive type A structures versus successive integers.

optical axis of the cavity. The power spectrum consists of a series of harmonics that are integer multiples of the pulse repetition rate: $f_n=nf_L$, where n is an integer and f_n is the harmonic frequency. The power spectrum of the acoustic wave is determined by the properties of the cavity, as well as by the driving source term of the laser discharge and the discharge medium properties. The pressure spectrum is, in general, complicated, since for a single pulse repetition rate there are a large number of acoustic wave frequencies, while for an enclosed cavity there are a large number of resonant frequencies. For small pulse repetition rates many harmonics can lie within the frequency range of a resonance, whereas for large pulse repetition rates, only one specific harmonic may be capable of exciting the resonance. Thus a specific cavity resonance can be excited by either a high harmonic of a low pulse repetition rate or a low harmonic of a high pulse repetition rate.

We have investigated the spatial distribution of the acoustic wave amplitude along the optical axis, transverse to the gas flow, by moving the pressure monitor along the axis of the electrodes. Clear standing-wave structures with pressure perturbation envelope and minima fixed in space could be detected, roughly consistent with the visually observed structure shown in Fig. 4. Looking at the spatial structure of higher-frequency resonances, one finds that the pressure distribution is not dominated by a single frequency, but rather there appear standing waves over a wide range of frequencies. Similar studies were done by moving the probe in the gas flow direction and observing the longitudinal mode structure. Dominant longitudinal cavity resonances around 1000 Hz and as high as 2500 Hz, similar to those appearing in the transverse pressure studies, have been observed.

Acoustic resonances in a cylindrical cavity are determined by the boundary conditions at the walls. In the transverse direction, along the optical axis, the resonant frequencies are therefore given by

$$f_m = \frac{mv}{2L}, \tag{1}$$

where m is an integer, L is the cavity length along the optical axis, and v is the speed of the acoustic wave in the discharge, given by

$$v = \left(\frac{\gamma RT}{M}\right)^{1/2}, \tag{2}$$

where T is the discharge temperature, R is the universal gas constant, γ is the ratio of specific heats of the medium at constant pressure and constant volume, and M is the effective molecular mass of the medium, equal to the weighted average by mole fraction of the molecular masses of each species constituting the gas mix.

On the other hand, if repetitive obstructions are present in the cavity, the dominant boundary conditions are given by the multiple nodes introduced by these at their separations rather than the end walls. If these structures are separated by a distance l and they create nodes at every n'th structure, then an integer number of half wavelengths must fit within a distance nl, leading to resonant frequencies given by

$$f_m = \frac{mv}{2nl}. \tag{3}$$

From the previous discussion we note that type A structures have $n=1$, type B structures have $n=2$, and type C structures $n=3$. Thus Eq. (3) can be verified experimentally by observing the laser frequencies at which a given structure type occurs. While Eq. (1) predicts a linear relationship between f_m and n for standing cavity waves, Eq. (3) does so between $1/f_m$ and n for the case of repetitive structures. The experimental results in Fig. 6 demonstrate clearly a linear relationship between $1/f_m$ and n. Since the slope is also proportional to $\sqrt{M}$, the 36% CO_2 gas mix trend has a steeper slope than that of the 10% CO_2 gas mix. The predicted cavity resonant frequencies calculated from Eq. (1) using the parameters of the current laser system—$L=100$ cm and acoustic wave speeds of 585 and 354 ms^{-1} for gas mixtures of 10:10:80 and 35:20:44, respectively—do not agree with the experiment. However, one finds very good agreement with the physical

Fig. 7 Slotted discharge electrode as viewed from (a) top and (b) bottom. The electrode employs slots of 1.5-mm width cut at a pitch of 4 mm and is hollowed to allow for a suitable damping material to be inserted.

feedthrough separation of $l=50$ mm, indicating the dominance of the repetitive structures on resonant frequencies, as given by Eq. (3).

We wish to report that acoustic wave phenomena also have a strong influence on the discharge development. This has been verified by a simple one-dimensional discharge model. The change of the discharge electron density n_e can be expressed by the relationship

$$e\frac{\mathrm{d}n_e}{\mathrm{d}t} = v_d n_e(\alpha-\beta) - n_e^2\gamma + S(t), \tag{4}$$

where e is the electron charge, v_d the electron drift velocity, and α, β, and γ the ionization, attachment, and recombination coefficients, respectively. The source term $S(t)$ describes the preionization by an external ultraviolet source. The growth of the discharge current $i(t)$ is given by

$$i(t) = en_e v_d A \tag{5}$$

with the discharge area A. The electron transport parameters can be extracted from Ref. 11. The model indicates that small pressure perturbations of only 1% to 2% can introduce changes in the discharge current of up to a factor 2 in the affected electrode area. Pressure disturbances of up to 4% have been measured in the strongest acoustic resonances, which can explain the observed discharge structures and also the observed discharge arcing. In addition there is feedback between the spatially nonuniform discharge and the standing acoustic wave, enhancing the effects.

4 Effect and Suppression of Acoustic Waves

Acoustic waves and the resulting nonuniform discharges have a strong effect on laser performance through changes in the laser gain. In this section we consider the effect of acoustic waves on the laser parameters, such as laser beam quality (M^2), small-signal gain, output power, and energy as well as output energy variation (jitter), and discuss means to suppress the effect of these waves.

4.1 *Suppression of Acoustic Waves*

It is possible to reduce the effect of acoustic waves inside the laser cavity on the laser output parameters by a number of measures. The amplitude of the generated acoustic waves can be reduced by spoiling the acoustic resonance conditions; the waves can be attenuated by placing acoustic absorbing materials inside the laser vessel; and the laser can be operated under conditions where it is less susceptible to acoustic disturbances. While acoustic waves cannot be eliminated entirely, their influence on the laser output can be reduced significantly and in some cases made negligible.[3,5] As a trivial solution, an operating regime can be chosen where no acoustic problems manifest themselves, such as at very low repetition rates, with lean gas mixes, or in frequency regions between resonances. This is, however, not always practical or even possible.

Since the acoustic waves are a result of harmonic enhancement through resonance inside the laser cavity, a way to reduce their influence is to reduce the resonant addition of these waves. Such a solution was implemented by varying the repetition rate randomly in a narrow band around a chosen operating point (the desired repetition rate).[12] The distribution of repetition rates was such that the mean repetition rate equaled the desired value, so that on average the power output from the laser was not different to the case of running continuously at the chosen fixed repetition rate. Using this technique will only be possible in applications where the timing aspect of the laser pulses is not important and only the average power of the laser is used, as in materials processing.

Finally, it is possible to reduce the amplitude of the various acoustic harmonics by damping the waves as they propagate back and forth along the various propagation axes. In the case of acoustic waves propagating normal to the electrodes, damping can be affected by slotting the electrode surface, thereby making it semipenetrable to the waves. The electrode is then hollowed out and the back volume filled with acoustic-wave-absorbing materials (e.g., porous metals, ceramics, or felt metals). This arrangement results in effective absorption and attenuation of the primary shock wave generated by the discharge and greatly reduces standing acoustic waves. Surprisingly, the glow discharge uniformity does not degrade due to the change in electrode surface as long as the transverse profile of the electrodes is maintained (i.e., the designed electrode profile is machined first and slots cut afterwards). An example of a slotted electrode is shown in Fig. 7. Standing acoustic waves (duct oscillations) can also be reduced by placing dedicated shock-absorbing acoustic panels on exposed walls of the laser chamber.

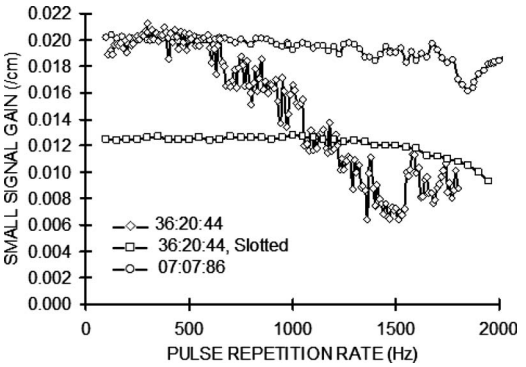

Fig. 8 Small-signal gain of the 2000-Hz laser amplifier versus repetition rate. There is a significant drop in gain at higher repetition rate when operating with a rich gas mix, due to acoustic activity. The efficacy of the slotted-electrode damping solution is clearly illustrated: The gain level is maintained even at high repetition rates.

4.2 *Effect on Laser Performance*

Figure 8 shows a plot of the small-signal gain as a function of laser repetition rate. As discussed earlier, at low repetition rates acoustic activity is low, but it increases with increasing repetition rate. Thus the deviation from a flat response at higher repetition rates can be attributed to the presence of acoustic waves. The small-signal gain of the high-repetition-rate laser measured in the original state without any acoustic-wave damping measures is shown in Fig. 8. The output is relatively stable, with small fluctuations, for the lean gas mixture 7:7:86. The rich 36:20:44 gas mixture, however, shows strong resonant behavior, with the gain at 1100 Hz dropping to one-third of its starting value. The position of the resonances is very reproducible, as confirmed by repeated scans. There is a marked decrease in the acoustic-wave influence when slotted electrodes are employed, with a near-flat response across all repetition rates even for the rich gas mix. This is also evident in Fig. 9, where the pulse-to-pulse energy jitter of the system due to acoustic waves both with and without slotted electrodes is shown. Also shown in Fig. 9 is the effect of the random-repetition-rate solution, which dramatically reduced the acoustic amplitudes.

Similar resonant behavior can be seen in the beam quality of the laser, as defined by the parameter M^2. The measurements shown in Fig. 10 were performed on a high-repetition-rate oscillator of similar design to the high-repetition-rate laser, but with reduced excitation energy. It employed a resonator consisting of a 15-m-radius-of-curvature back reflector with 100% reflectivity and a flat 36%-reflectivity output coupler. Because both the beam quality and the laser output power decrease at the acoustic resonances, the overall laser brightness is severely affected by acoustic waves.

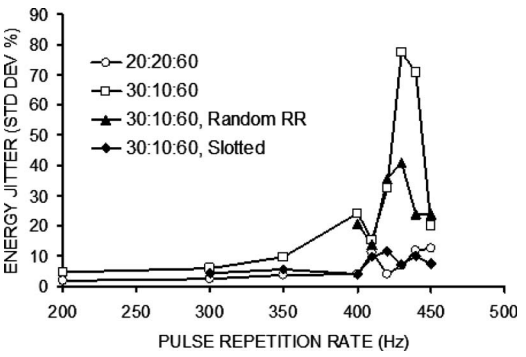

Fig. 9 Laser output energy jitter versus repetition rate, showing the reduction in jitter when the random-repetition-rate solution is implemented, as well as when the slotted electrodes are used.

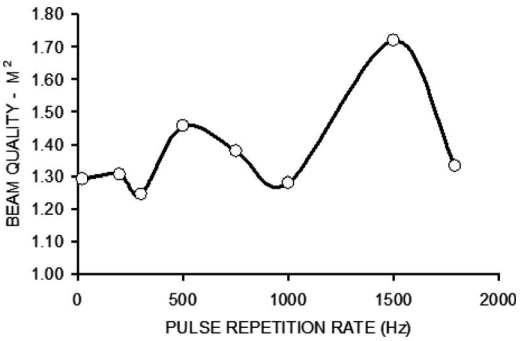

Fig. 10 Laser beam quality factor M^2 of the laser resonator versus pulse repetition rate.

5 Conclusion

We have presented experimental results on the effect of acoustic waves on the output laser beam of high-repetition-rate TEA CO_2 lasers. At the pulse repetition rates that lead to resonant conditions inside the cavity for the acoustic waves, one finds deleterious effects on the laser gain and discharge uniformity, leading to decreased output energy, a worsening of the laser beam quality, and an increase in pulse-to-pulse energy variation. The implementation of acoustic-wave damping measures such as slotted electrodes and/or operating the laser at randomly varied repetition rates was shown to decrease the effect of the acoustic waves.

Acknowledgments

The authors would like to gratefully acknowledge the opportunity to work on this topic provided by Scientific Development and Integration (Pty) Ltd. as well as the Nuclear Energy Corporation of South Africa (NECSA).

References

1. V. Y. Baranov, D. P. Malyuta, V. S. Mezhevov, and A. P. Napartovich, "Superheating-acoustic instability in periodic-pulsed lasers," *Sov. J. Plasma Phys.* **6**(4), 428–432 (1980).
2. V. Y. Baranov, S. A. Kazsakov, D. D. Malyuta, V. S. Mezhevov, A. P. Napartovich, V. G. Nisiev, M. Y. Orlov, A. I. Starodubtsev, and A. N. Starostin, "Average power limitations in high-repetition-rate pulsed gas lasers at 10.6 and 16 μm," *Appl. Opt.* **19**(6), 930–936 (1980).
3. J. P. Truong, M. L. Sentis, P. C. Delaporte, B. M. Forestier, B. L. Fontaine, O. P. Uteza, and I. Tassy, "Efficient acoustic wave damping in a high pulse repetition rate XeCl laser," *Proc. SPIE* **1810**, 430–434 (1992).
4. C. J. Knight, "Transverse acoustic waves in pulsed lasers," *AIAA J.* **20**(7), 933–939 (1982).
5. V. A. Kulkarny, "Decay of transverse acoustic waves in a pulsed gas laser," *AIAA J.* **18**(1), 1336–1341 (1980).
6. A. Forbes, L. R. Botha, N. du Preez, and T. E. Drake, "Design and optimisation of a pulsed CO_2 laser for laser ultrasonic applications," *S. Afr. J. Sci.* **102**, 329–334 (2006).
7. A. Forbes and L. R. Botha, "Predicting gas decomposition in an

industrialized pulsed CO_2 laser," *Proc. SPIE* **5777**, 491–494 (2005).
8. A. Forbes, L. R. Botha, N. du Preez, and T. E. Drake, "Influence of laser parameters on laser ultrasonic efficiency," *Proc. SPIE* **6346**, 63462X1 (2007).
9. O. P. Uteza, P. C. Delaporte, B. L. Fontaine, B. Forestier, M. L. Sentis, I. Tassy, and J. P. Truong, "Acoustic wave origin in excimer lasers," *Appl. Phys. B: Lasers Opt.* **B64**, 531–537 (1997).
10. H. M. von Bergmann, G. L. Bredenkamp, and P. H. Swart, "High repetition rate high power excimer lasers," *Proc. SPIE* **1023**, 20–24 (1988).
11. J. J. Lowke, A. V. Phelps, and B. W. Irwin, "Predicted electron transport coefficients and operating characteristics of CO_2-N_2-He laser," *J. Appl. Phys.*. **44**, 4664–4671 (1973).
12. H. M. von Bergmann, A. Forbes, T. Roberts, and L. R. Botha, "Influence of acoustic waves on TEA CO_2 laser performance," *Proc. SPIE* **6346**, 6346061 (2007).

Hubertus M. von Bergmann received an MSc degree in physics from Kiel University, Kiel, Germany and a PhD in laser physics from the University of Natal, Pietermaritzburg, South Africa, in 1973 and 1980, respectively. He has carried out research on high-repetition-rate, high-power excimer and CO_2 TEA lasers at Lambda Physik GmbH, Göttingen, Germany, the National Physical Research Laboratory of the CSIR in Pretoria, South Africa, and the Systems Laboratory of the Rand Afrikaans University in Johannesburg. From 1991 to 1999 he was part of the AEC Molecular Laser Isotope Separation (MLIS) project and the National Laser Facility in Pretoria. He joined the Physics Department of the University of Stellenbosch, Stellenbosch, South Africa, in January 2000, where he is now full professor in laser physics.

Andrew Forbes received his BSc (physics/mathematics) in 1990, BSc Hons (physics) in 1991, and PhD (physics) in 1998 from the University of Natal, Durban (South Africa). His doctoral thesis considered photothermal effects due to high-power laser beams. He has spent several years working as an applied laser physicist on high-power lasers for the MLIS process for uranium enrichment, and then later on gas lasers for laser ultrasonic applications. He is presently a principal researcher at the CSIR National Laser Center (Pretoria, South Africa) and is the research group leader for the Mathematical Optics Group. His research interests include laser beam propagation, wavefront control for laser beam shaping, and laser resonator analysis and design. He is chair of the SPIE Laser Beam Shaping Conference, and is an active member of SPIE and the South African Institute of Physics.

Ted Roberts obtained his BSc and PhD degrees at Imperial College, London University. He subsequently spent a year at the Institute for Aerospace Studies in Toronto, Canada, followed by two years at the University of British Columbia in Canada. This was followed by two years on the high-current arc project at the University of Liverpool, England, and then time in the Food Research Department of the CSIRO in Australia and the Cancer Research Unit of the Institut Jules Bordet in Belgium. Most of his working life was then spent on the study of magnetic instabilities in the tokamak at the Atomic Energy Corporation (AEC) of South Africa. After this, three years were spent on the Molecular Laser Isotope Separation (MLIS) program at the AEC before joining the newly formed National Laser Centre (NLC) of South Africa, where he has worked on a variety of projects, including laser paint stripping; nuclear decontamination of surfaces using lasers; lidar, including detection of biological volatile organic compounds (BVOCs); and recently the newly established femtosecond laser facility.

Lourens R. Botha received BSc (Hons) and MSc (physics) degrees from the University of Pretoria, and a PhD in physics from the University of Natal in Durban. He was employed by the Atomic Energy Corporation of South Africa from 1984 to 1997. He was a founding member of a laser company Scientific Development and Integration and was a director of this company from 1997 to 2004. He is currently employed by the CSIR National Laser Centre in Pretoria, South Africa, where he is the manager of the Laser Physics and Technology Group. His current research interests are femtosecond science and in particular coherent control of complex systems.